DESY Summer Student 2011

A catalogue of potential ν-signals of galactic γ-ray sources

IceCube

Author: Basho Kaminsky

Supervisor: Alexander Kappes
Markus Ackermann

Abstract

A source catalogue of potential neutrino sources in our galaxy from observed gamma rays is created. The gamma data was taken from different gamma ray observatories: FERMI, HESS, MAGIC, VERITAS. The expected neutrino flux is calculated by assuming hadronic production of the gamma rays. Finally the expected event rate in two neutrino telescopes (IceCube and KM3NeT) is computed with respect to the detector properties.
The results will be published in a online catalogue. The methods used in this project follow the work done by Kappes et al.: "Potential neutrino signals from galactic γ-ray sources" (Kappes et al. [2007]).

1 Introduction

The development of neutrino and gamma ray astroparticle physics in the last years was quite impressive.
New telescopes and observation experiments were conceived and constructed. One of the new telescopes is the IceCube neutrino detector. IceCube detects neutrinos in a wide energy range and with its large detector volume, the possibility to see neutrinos from individual sources increases.

The sources widely vary in their nature. They can be anything from extragalactic phenomena like AGN[1] to sources in the milky way. The sources in our own galaxy cover again a wide range of different phenomena. There are High Mass Binaries, Supernova remnants, pulsar wind nebulae and other sources of high energy particles. These sources may produce high-energy neutrinos due to the interactions of high-energy protons. Large detector volumes are necessary, because neutrinos are weakly interacting particles.
All of these source classes also emit high-energy gamma-rays which have been observed by ground and satellite based gamma-ray telescopes. Ground based telescope like imaging atmospheric Cherenkov telescopes, e.g. HESS[2], MAGIC[3] or VERITAS[4] observe Cherenkov light from gamma-ray induced air showers.
Due to the fact that nearly all gamma rays are absorbed in the atmosphere, another important branch of gamma ray observations are satellite missions. One of these satellite projects is the FERMI Gamma-ray Space Telescope[5].

To learn something about the production and acceleration processes in the sources, it is interesting to compare the ν- and γ-flux.
The target of this project is to determine the expected ν-flux for a known γ-flux assuming that the underlying particle acceleration process is hadronic, i.e. that the gamma rays are exclusively produced in the interactions of high-energy protons. For the expected ν-flux, the detector characteristics were taken in consideration. For the source parametrization of the high-energy proton spectrum in the source, a power law with exponential cutoff is chosen(Kelner et al. [2006]).
The idea of this project is based on the work "Potential neutrino signals from galactic gamma-ray sources" (Kappes et al. [2007]). It was realized during the DESY Summer Student Program 2011.

[1] Active Galactic Nuclei
[2] High Energy Stereoscopic System
[3] Major Atmospheric Gamma-Ray Imaging Cherenkov Telescopes
[4] Very Energetic Radiation Imaging Telescope Array System
[5] former GLAST, Gamma-ray Large Area Space Telescope

2 Fundamentals

2.1 Galactic gamma ray and potential neutrino sources

The Milky Way shows a variety of different gamma ray sources. The most important sources for this work are:

- Supernova Remnants (SNR)
- High Mass Binaries (HMB)
- Pulsar Wind Nebulae (PWN)

SNRs are nebulae resulting from a supernova. A shockwave ejects material with velocities around $10^5 \frac{\mathrm{m}}{\mathrm{s}}$ and creates mostly a shell like structure. The ambient medium slows down the ejected gas and the plasma can reach temperatures in the range of 10^7 up to 10^8 K. The shell itself can be cooled down, encasing the hot material inside. The detection of TeV γ-rays from the shell of SNRs provides evidence that effective particle acceleration occurs within.
Accelerated electrons and protons emit gamma rays and neutrinos through inverse Compton scattering of relativistic electrons, bremsstrahlung and the production and decay of pions. The inverse Compton scattering appears if TeV-electrons scatter on photon fields like the cosmic microwave background (CMB). RX J1713.7–3946 is an example where most of the high-energy gamma-ray emission is assumed to originate from IC. This SNR has a flux comparable with the Crab nebulae around one TeV.

HMBs are binary systems of a massive star and a compact object like a neutron star or a black hole. They are also called X-Ray HMB, because they emit light in the X-ray range. If they only have a normal star as stellar component, they are called X-Ray Binaries. A binary object with a strong and variable radio emission is called a microquasar. They have relativistic jets which accelerates particles to energies up to TeV (Aharonian et al. [2005b]). In those systems cooling of TeV electrons is very effective due to the high density of the radiation, so the gamma ray emission might be of hadronic origin. This makes them promising neutrino sources.
An example is the X-Ray binary LS 5039, which was identified as an TeV γ ray emitter with HESS (Aharonian et al. [2005b]).

PWNs are nebulae with a pulsar[6] in its centre. The emissions of the nebula are caused by the pulsar wind which provoke shock waves in the nebula surrounding medium. They represent some of the brightest sources in the TeV gamma ray range. The main emission mechanism is considered to be inverse Compton Scattering of high energy electrons on γs, for example on CMB photons, but high-energy nuclei may also be present and produce non-negligible neutrino and gamma-ray fluxes through the decay of pions.
A good example for PWNs is the bright Crab PWN. This two kpc distant source was created by the supernovae SN1054 and is powered by the Crab Pulsar.

As well as the cosmic ray spectrum there is a cosmic neutrino spectrum (see figure 2, with values from Frejus[7] and AMANDA[8]) that originates from neutrinos produced by cosmic processes. Here, the focus is mainly on neutrinos from galactic sources.

[6] Rotating magnetized neutron star.
[7] High-resolution iron calorimeter in France.
[8] Antarctic Muon and Neutrino Detector Array, 1997 - 2005, now integrated in IceCube

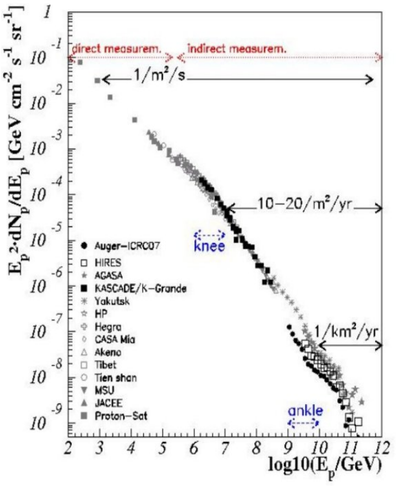

Figure 1: Cosmic γ ray spectrum (Berger [2008]), containing γ from all production mechanism. Values belong to different experiments.

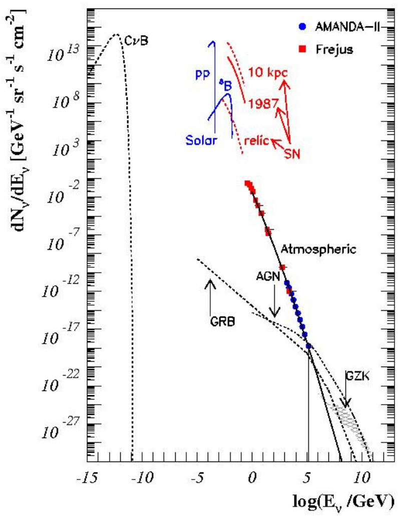

Figure 2: Cosmic ν-spectrum (Berger [2008]), containing ν of cosmological origin, sun, atmospheric, SN, AGN and GZK ν. The dashed lines base on hypothesis and the solid lines were shown by measurements.

The main neutrino production process is the decay of pions, which are produced in inelastic pp-interactions with the surrounding medium. The π can decay for example into a muon and a muon neutrino, and the muons can afterwards decay again into an electron or a positron and the associated neutrino. Another decay channel of the pion is into two photons that can be detected as gamma rays. Yet another production process in supernovae is: $e^- + p \rightarrow n + \nu_e$ or $e + e \rightarrow \nu + \bar{\nu}$ The spectra of the secondary particles depend on the primary proton spectrum and the processes like diffraction that one must take into account, which makes spectra for example harder (Kamae et al.[2006]). More details on modelling used in this work are in section 3. There are also other source types and sources with no counterpart in other wavelengths. So there are diffuse emissions from galactic plane from unresolved sources. Also, giant molecular clouds seem to emit gamma rays (Aharonian et al. [2006a]).
Furthermore, sources with a very hard spectrum exist. These sources are not detectable in the energy range above ∼10 TeV with actual gamma ray telescopes, but they are promising objects for the detection with neutrino telescopes, because the effective area rises steeply with energy.

2.2 Observation missions

Most observational data used in this work originates from imaging Cherenkov air shower telescopes.
HESS is an array of four of these telescopes, located in Namibia. It has an angular resolution below 0.1° and can observe gamma rays of 100 GeV and 100 TeV with an energy resolution of about 15%. It consists of four telescopes from which each has a 12 m diameter. The mirror is composed of 382 small mirrors and the 5° field of view camera consists of

960 photon detectors.
MAGIC is also an array of two air shower telescopes. It is located on the Canary Islands and has an active mirror surface of 236^2 m. The sensitive energy range is 0.025 - 30 TeV and it has an angular resolution of also 0.1°.
VERITAS is an array of 4 gamma ray telescopes and located in South Arizona. The resolution is $\lesssim 0.15°$ and the main sensitivity is between 100 GeV and 10 TeV. The single telescopes have a 12 m reflector constructed from 350 single mirrors and a 499 pixel camera. It has an 3.5° field of view.

Other data belong to the FERMI satellite mission. The FERMI mission started in 2008. It carries two main instruments. The first one is the GLAST Burst Monitor, which observes with a field of view of 4π with two scintillation detectors the energy range of 150 keV up to 30 MeV. The other instrument, which is the main FERMI instrument, delivers the used data. The Large Area Telescope (LAT) energy range is between 20 MeV and 300 GeV. It is an imaging instrument with an angular resolution highly dependent on the energy: 3° at 100 MeV, 0.04° at 100 GeV. It also provides spectral information due to the fact that it is not only constructed from a tracker (silicon strip detectors), but is also a calorimeter (cesium iodide calorimeter). The LAT field of view is 2.4 sr.

The neutrino flux is calculated for two neutrino telescopes, the current generation IceCube and the next generation KM3NeT detectors. An example of how the sky looks like for a neutrino observatory is shown in figure 3.

The neutrino flight direction can be computed from the three dimensional grid of detectors, which provides together with the energy and flux the probability to compute an image.

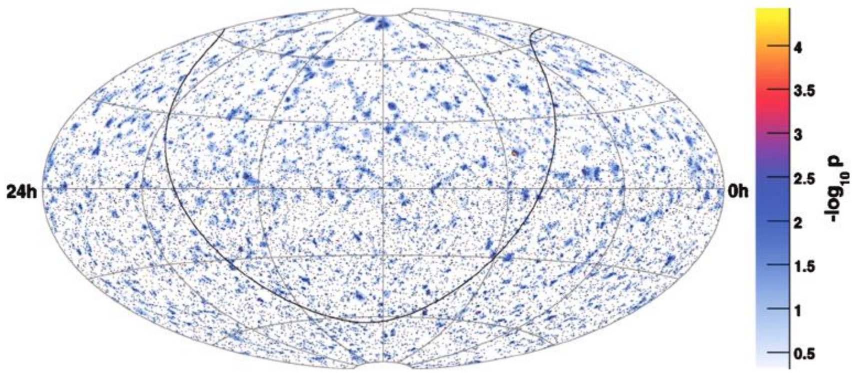

Figure 3: Neutrino sky for IceCube with 40 strings (Halzen & Klein [2010]). The figure shows the point source probability for 0.1 TeV - some 100 TeV operating for $\frac{1}{2}$ year.

Another smaller current generation neutrino telescope is ANTARES[9], a water Cerenkov detector located in the Mediterranean Sea. The expected event rate was calculated by A. Kappes et al. ([2007]). They found a very low event rate, so that a detection with ANTARES is very unlikely. For this reason the calculations were not done for ANTARES again.
The IceCube detector at the south pole offers a higher possibility for detection. It detects the Cherenkov light emitted by charged particles, like electrons, muons or taus, which are created by interactions of neutrinos. The detector uses a volume of 1 km^3 and works with a photomultiplier inside the so called DOMs (digital optical module). The 5160 DOMs are

[9]Astronomy with a Neutrino Telescope and Abyss environmental RESearch.

up to 2450 m below the surface, where the ice is very clear, and distributed over 86 strings and an area of 1 km^2. The detectors are sensitive enough to detect single photon events and provide a time resolution of 5 ns. The observable energy range goes from a 100 GeV threshold up to PeV and the angular resolution is better than 1° throughout most of the energy range. On the surface above the detector is the IceTop experiment, which detects Cherenkov air showers in the range of TeV up to EeV.
Future neutrino telescopes like KM3NeT can offer a higher possibility to find galactic sources due to its position in the Northern Hemisphere. KM3NeT is planned in the Mediterranean Sea with a km^3 detector volume. The angular resolution is planned to be better than 0.1° for energies above 10 TeV. The detector will be able to observe all three neutrino flavors and will have a few hundreds of GeV threshold. It will offer the possibility to observe the larger part of our galaxy including the galactic centre. The design study was published in 2009 and the technical design report was published in 2011. The construction is expected to start in 2012 and when completed, KM3NeT will complete IceCube observations.

3 Neutrino production model

High-energy neutrinos are produced in interactions of protons with ambient protons and photons. In these interactions charged and neutral pions are produced which then decay into gamma rays (neutral pion) or neutrinos and charged leptons (charged pions). Assuming this is the dominant process for production of high-energy gamma-rays for a given source , this makes it possible to derived from the used model (Kappes et al. [2007]) the expected ν-spectra from the γ-spectra. For the energy range covered by neutrino telescopes, one expects curved spectra. Here, as parametrization of the proton and secondary particles spectra, a power law with an exponential cutoff is used. These parametrizations yield the expected γ- and ν-spectra (Kelner et al. [2006]). The assumptions made are that there is no appreciable absorption inside the source for γ- and ν, that the pions decay without interacting before and that the source is distant enough for full neutrino mixing. Those assumptions have been derived for energies above 100 GeV. So the resulting γ- and ν-spectra are described by a power law with an exponential cutoff:

$$\frac{dN_\beta}{dE_\beta} \approx k_\beta \left(\frac{E_\beta}{1\text{TeV}}\right)^{-\Gamma_\beta} \exp\left(-\sqrt{\frac{E_\beta}{\epsilon_\beta}}\right) \tag{1}$$

with $\beta = \{\gamma, \nu\}$, E_α is the energy and:

$$k_\nu \approx (0.71 - 0.16\alpha)\, k_\gamma \tag{2}$$

$$\Gamma_\nu \approx \Gamma_\gamma \approx \alpha - 0.1 \tag{3}$$

$$\epsilon_\nu \approx 0.59\, \epsilon_\gamma \approx \frac{\epsilon_p}{40} \,. \tag{4}$$

α is here the power law index of the primary proton spectrum. This model assumes a production ratio between electron- and μ-neutrinos of 1:2. It also considers a neutrino mixing, so that only a fraction of $\frac{1}{3}$ of the source flux can be measured. A pure power law can also be calculated with this model with a cutoff energy $\epsilon_\beta = \infty$. Equation 1 gives the spectra on Earth.
The properties of the detector that were taken into account are described in the next section.

4 Neutrino detector properties

The measurable event rate depends on the spectrum, the effective area of the detector, the background rate and the visibility of the source for the detector. The visibility has an especially great influence for IceCube if one tries to observe galactic sources.
A way to compare the different abilities of (neutrino) detectors is the *effective area*. The number of detected events depends on the geometry of the detector, the energy of the detected particle, the angle of the incoming neutrino and the properties of the detector surrounding medium. The effective area is then the area a detector would have if one sees the same fixed number of events compared with a beam hitting the detector area normal and if the detector has a 100% efficiency. For a given number of detected events N, and for a given flux F, the effective area A_{eff} is defined as:

$$N = \int\int\int dt\, d\omega\, dE\, F(t, E, \omega) \cdot A_{eff}(E, \omega) \tag{5}$$

with the solid angle ω, the energy E and time t. From this equation it follows for a real detector with the area A_R and a number of incoming particles N_R for the effective area:

$$A_{eff} = \frac{N \cdot A_R}{N_R} \tag{6}$$

The muons from interactions of cosmic rays in the Earth's atmosphere provide a disruptive background for the detector. The flux from these interactions of cosmic rays in the atmosphere is orders of magnitude higher than the original neutrino flux. For that reason, the Earth is used as a filter, which means that the neutrino telescopes observe through the hemishpere of the sky which is shielded by the Earth. This implies the existence of features like additional attenuation and conversion of neutrino flavours. These features have an influence on the effective area.

The following calculations were adopted from Kappes et al. [2007].
For a given neutrino flux F_ν it then follows for the event rate in the detector:

$$\frac{dN_\nu}{dt} = \int dE_\nu\ A_{eff\nu}\, F_\nu \tag{7}$$

The resulting effective area is energy and direction dependent and different for all detectors.

Both neutrino telescopes show an energy threshold similar to the threshold of the imaging Cherenkov air shower telescopes.
The threshold and energy range of FERMI is for the most part below the threshold of the neutrino telescopes.
The energy resolution and uncertainty of the neutrino telescopes is here neglected and the data assumed to be the exact neutrino energy.

The point spread function (PSF) of the neutrino detectors and the PSF of the optical determined position of an object gives the search window for the object in the neutrino detector. If one deals with extended sources, one has to consider also the shape of the source. Due to the effect that one loses neutrinos that are scattered outside the search window, one assumes a correction factor of 0.72 that reduces the number of expected events.

One can calculate the expected number of detected events with:

$$N_\nu = 0.72 \cdot \int dt\, \frac{dN_\nu}{dt} \tag{8}$$

The integration limits are given by the time when the source is below the horizon.
An example for the effective area for KM3NeT shown in figure 4.

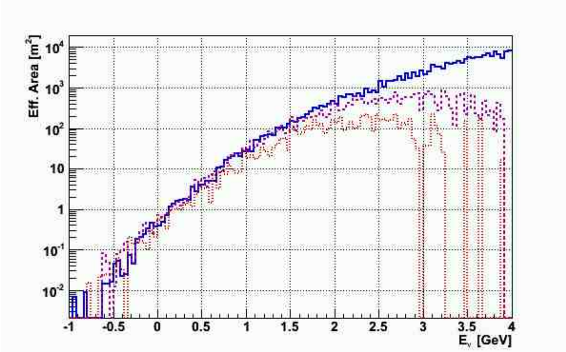

Figure 4: Effective area plot for KM3NeT for three different zenith angles: 90° (blue), 130° (magenta) and 180° (red).

5 Source catalogue

The source catalogue contains the data from the 3 imaging Cherenkov air shower telescopes and from FERMI. For a short description of the observation missions see section 2.2.
It contains sources which are located in our galaxy and were classified as one of the three source types described in section 2.1: HMB, PWN or SNR. Note that the source classification also has an uncertainty.
The raw catalogue contains at the moment 107 sources, where sources can appear multiple times if they were observed by more than one observation mission. 57 sources were observed by HESS, 18 by MAGIC and 9 by VERITAS. The spectral data from FERMI are taken from publications from the FERMI collaboration (#13) and from the FERMI LAT 2-Year Source Catalog[10] (2FGL) (#5). The spectral data from the 2FGL catalogue give originally the integral photon flux derived from the likelihood analysis with a power law. For our purpose, the differential flux is calculated from this values if no paper has been published for this source.

All calculations and values are, if not given otherwise, given in: TeV (energy) and $\frac{1}{\mathrm{TeV\,cm^2 s}}$. This is also valid for the online catalogue.

The complete source catalogue will be published in a online version together with the calculation results. The web page will be a static HTML site, though the catalogue and data sites are created with a program automatically if the catalogue is updated. This method is chosen due to the fact that there is no high update frequency, making a dynamically created page with database backend unnecessary. From the main catalogue site one can go to a sub page with detailed results for a specific source. On the sub page, one can find the results of the fit of the gamma spectrum, of the derived neutrino spectrum, a figure of the fit with the data and comments. An example is displayed in figure 5.

6 Results

The results for the sources contain several features. All calculations were performed for all objects in the catalogue with spectral data (sometimes missing spectra). In the case where the spectrum contains only upper limits, the calculation was done using the upper limits as a hypothetical maximum flux to show the maximum allowed neutrino flux for

[10] Covering energies from 100 MeV up to 100 GeV

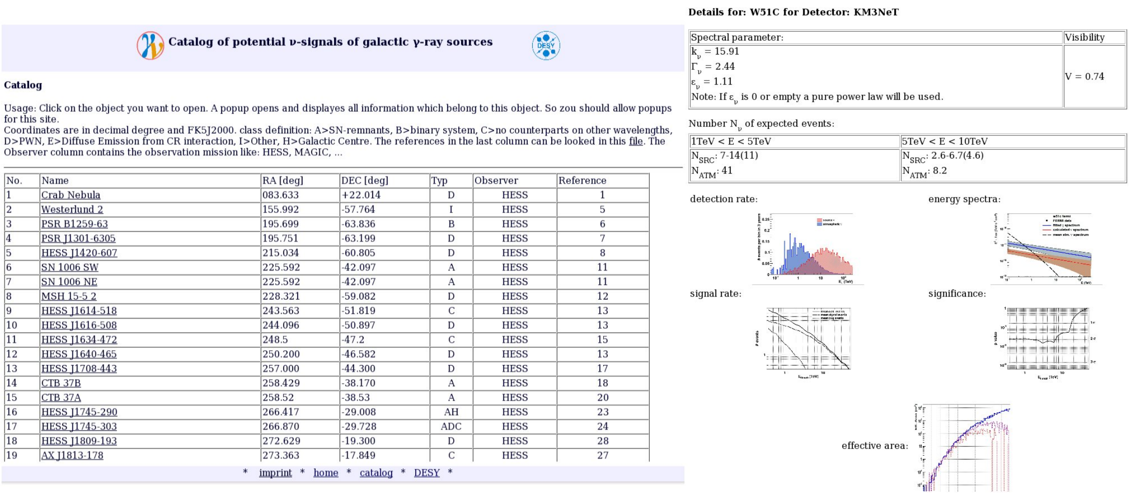

Catalog of potential ν-signals of galactic γ-ray sources

Catalog

Usage: Click on the object you want to open. A popup opens and displayes all information which belong to this object. So zou should allow popups for this site.
Coordinates are in decimal degree and FK5J2000. class definition: A>SN-remnants, B>binary system, C>no counterparts on other wavelengths, D>PWN, E>Diffuse Emission from CR interaction, I>Other, H>Galactic Centre. The references in the last column can be looked in this file. The Observer column contains the observation mission like: HESS, MAGIC, ...

No.	Name	RA [deg]	DEC [deg]	Typ	Observer	Reference
1	Crab Nebula	083.633	+22.014	D	HESS	1
2	Westerlund 2	155.992	-57.764	I	HESS	5
3	PSR B1259-63	195.699	-63.836	B	HESS	6
4	PSR J1301-6305	195.751	-63.199	D	HESS	7
5	HESS J1420-607	215.034	-60.805	D	HESS	8
6	SN 1006 SW	225.592	-42.097	A	HESS	11
7	SN 1006 NE	225.592	-42.097	A	HESS	11
8	MSH 15-5 2	228.321	-59.082	D	HESS	12
9	HESS J1614-518	243.563	-51.819	C	HESS	13
10	HESS J1616-508	244.096	-50.897	D	HESS	13
11	HESS J1634-472	248.5	-47.2	C	HESS	15
12	HESS J1640-465	250.200	-46.582	D	HESS	13
13	HESS J1708-443	257.000	-44.300	D	HESS	17
14	CTB 37B	258.429	-38.170	A	HESS	18
15	CTB 37A	258.52	-38.53	A	HESS	20
16	HESS J1745-290	266.417	-29.008	AH	HESS	23
17	HESS J1745-303	266.870	-29.728	ADC	HESS	24
18	HESS J1809-193	272.629	-19.300	D	HESS	28
19	AX J1813-178	273.363	-17.849	C	HESS	27

* imprint * home * catalog * DESY *

Details for: W51C for Detector: KM3NeT

Spectral parameter:	Visibility
k_ν = 15.91 Γ_ν = 2.44 ε_ν = 1.11 Note: If ε_ν is 0 or empty a pure power law will be used.	V = 0.74

Number N_ν of expected events:

1TeV < E < 5TeV	5TeV < E < 10TeV
N_{SRC}: 7-14(11) N_{ATM}: 41	N_{SRC}: 2.6-6.7(4.6) N_{ATM}: 8.2

Figure 5: Left: Example how the catalogue web page looks like. Right: Example how the details web page for an object looks like.

this source.
The effective area has been plotted for three different zenith angles: 90°, 130° and 180°. The effective area for KM3NeT is shown in plot 4. The effective area for KM3NeT is a preliminary assumption. The effective area of IceCube is generated with Monte Carlo simulations and considers additional effects like the ice quality, the photon efficiency or quality of the triggered event.

The background spectrum and event rate is mainly caused by atmospheric neutrinos. Atmospheric neutrinos are produced by the interaction of cosmic rays with the atmosphere of the earth. The flux of atmospheric ν is also angle dependent.
The used parametrization of the atmospheric neutrino flux (Volkova [1980]) takes this angle and an energy dependency into account and works well for energies below 100 TeV.

6.1 Spectra

The calculation of the ν spectra is given in section 3. The data were taken from the publications given in the reference list (see the web catalogue). If the data points for the different γ ray telescopes do not fit smoothly enough, the expected fluxes were calculated individually for the telescopes.
The plot of the spectrum for a source contains the measured values for the γ ray spectrum, the fitted curve for it and for the ν-spectra the estimated curve. All values and curves are given with errors or, for curves, error regions. If no error is given, the values are upper limits or were generated from upper limit values. The error regions represent a 1σ uncertainty.
The plots show the flux multiplied by E^2 and show also the calculated atmospheric neutrino spectrum.
The values of spectral parameter ϵ_ν, k_ν and Γ_ν from equation 1 were given also in the catalogue like the number of expected mean ν events for the source for KM3NeT and IceCube.
One example for the spectra plot is shown in figure 6.

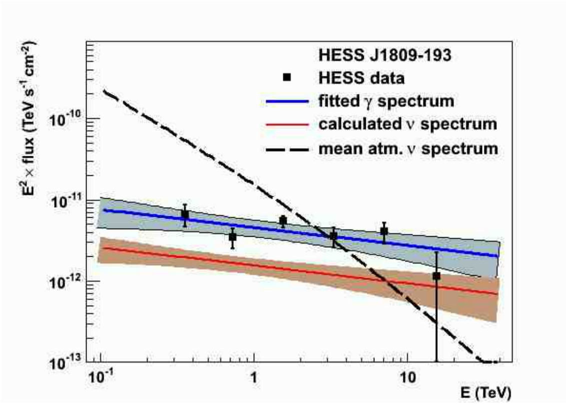

Figure 6: Example (HESS J1809-193 with HESS data, calculated for KM3NeT) of the resulting spectra plot, containing the atmospheric neutrino spectra, the data points from the γ-spectrum, the fit of the γ spectrum and the calculated ν spectrum.

6.2 Expected neutrino fluxes

The expected neutrino rates were calculated as shown in section 3 and 4.
The plot of the detection rates contains the expected ν event rate for the source neutrinos and the atmospheric neutrinos with respect to the detector properties as written in section 4. The event rates for the PWN HESS J1809-193 in a given observation time duration is shown in figure 7. For energies up to several TeV, the atmospheric event rate will be higher than the event rate generated by the object itself. A similar feature can be seen for the integrated event rate above a certain energy threshold shown in figure 8. In this plot, the number of events versus the energy threshold is visualized (see example figure 8). One can see that the number of events originating from the source increases with the rising threshold. Figure 9 shows the average significance of the detection that would be reached with the given signal and background event numbers.

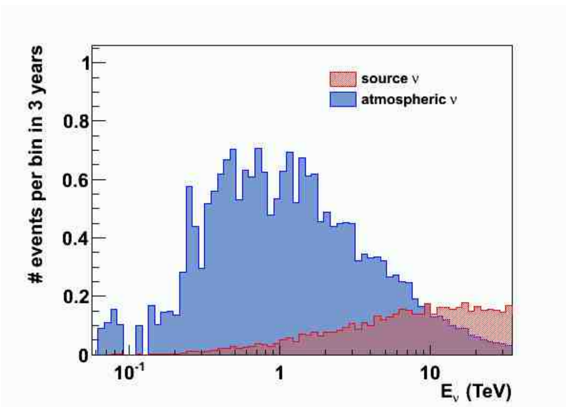

Figure 7: Example (HESS J1809-193 with HESS data, calculated for KM3NeT) of the resulting number of events during the observation time.

7 Discussion

With the resulting neutrino event rates of around several events during an observation time of a couple of years, it seems to be in principle possible to detect these objects

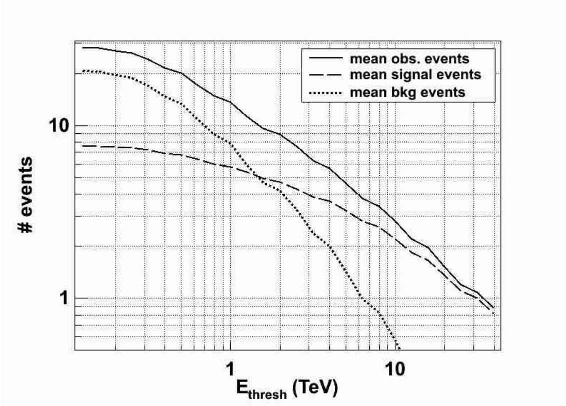

Figure 8: Example (HESS J1809-193 with HESS data, calculated for KM3NeT) of the resulting event rate as a function of threshold energy.

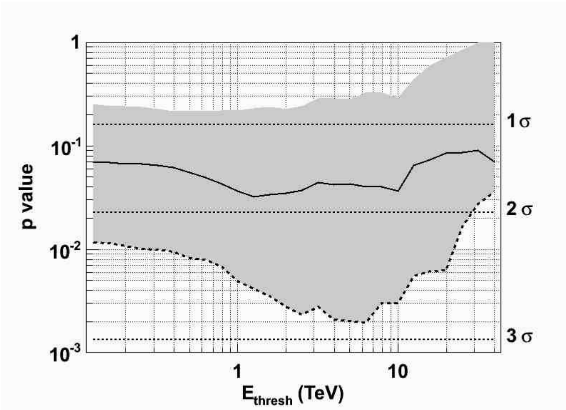

Figure 9: Example (HESS J1809-193 with HESS data, calculated for KM3NeT) of the resulting significance of source flux as a function of threshold energy.

with both ν telescopes, KM3NeT and IceCube. Together with the observations from the ν telescopes, it will be possible to compare the estimated fluxes with the observed one. With this comparison, there is a chance to measure if hadronic interaction processes are responsible for the bulk of the high-energy emission. There will be also the possibility to chose promising sources for the observation.

Due to the fact that the calculations were done with respect to detector and source properties like effective area or search window for the source, one can see the influences of several parameters on the observations. So for example the different numbers of expected events for both ν observatories. One feature here is the difference in visibility of a source for both detectors. This also shows how essential the future planned KM3NeT is as a counterpart to IceCube.

Acknowledgment

At first I want to thank the organizers for the great chance to join the Summer Student Programme of DESY. This made it possible for me gain a lot of new knowledge and experience. Especially Sabine Baer and Karl Jansen should be praised for the time, organization and help they provide.
For the great support I want to thank my supervisors, Markus Ackermann and Alexander Kappes. For proofreading I want to thank Nina Kudryashova.
But I also want to thank Christian Spiering and the rest of the IceCube group for their support and giving me the possibility to be a member of the group.
Last but not least I have to thank my Summer Student colleagues for the great time.

References

[2005a] Aharonian, F. A., et al. (H.E.S.S. Collaboration), 2005, A&A, 437, L7

[2005b] Aharonian, F. A., et al. (H.E.S.S. Collaboration), 2005, Science, 309, 746

[2006a] Aharonian, F. A., et al. (H.E.S.S. Collaboration), 2006, Nature, 439, 695

[2008] Becker, J. K., Phys. Rep. 458, 173 2008, arXiv:0710.1557

[2010] Halzen, F., Klein, S. R., 2010, doi:10.1063/1.3480478

[2006] Kamae, T., Karlsson, N., Mizuno, T., Abe, T., Koi, T., 2006, ApJ, 647, 692

[2007] Kappes, A., Hinton, J., Stegmann, C., Aharonian, F. A., 2007 , ApJ, 656, 870

[2006] Kelner, S. R., Aharonian, F. A., Bugayov, V. V., 2006, Phys. Rev. D, 74, 034018

[1980] Volkova, L. V. 1980, Soviet J. Nucl. Phys., 31, 784